IEEE Access
Multidisciplinary ⋮ Rapid Review ⋮ Open Access Journal

Received August 12, 2016, accepted September 6, 2016, date of publication September 13, 2016, date of current version September 28, 2016.

Digital Object Identifier 10.1109/ACCESS.2016.2608923

Joint Optimization of User Grouping and Transmitter Connection on Multi-Cell SNR Blind Interference Alignment

QING YANG[1], (Student Member, IEEE), TING JIANG[1], CHUNXIAO JIANG[2], (Senior Member, IEEE), ZHU HAN[3], (Fellow, IEEE), AND ZHENG ZHOU[1], (Member, IEEE)

[1]Key Laboratory of Universal Wireless Communication, Ministry of Education, Beijing University of Posts and Telecommunications, Beijing 100876, China
[2]Tsinghua Space Center, Tsinghua University, Beijing 100084, China
[3]Electrical and Computer Engineering Department, University of Houston, Houston, TX 77004, USA

Corresponding author: C. Jiang (chx.jiang@gmail.com)

This work was supported in part by NSFC China under Project 61371079 and in part by US NSF under Grant CPS-1646607, Grant ECCS-1547201, Grant CCF-1456921, Grant CNS-1443917, Grant ECCS-1405121, and Grant NSFC61428101.

ABSTRACT Blind interference alignment (BIA) can greatly improve the degree of freedom with the infinite signal-to-noise ratio (SNR) assumption. Under the finite SNR condition, noise accumulation can have a significantly negative impact on SNR, inducing severe performance deterioration. In particular, in multi-cell networks, the transmitter to which a user connects can further affect its received SNR and the BIA design. To address such problem, we present a user grouping scheme for reducing noise accumulation in a single cell and analyze the impact of transmitter connections on the user grouping scheme. SNR BIA in a multi-cell network is further proposed, which jointly optimizes the transmitter connection and the user grouping scheme. Extensive simulations demonstrate that the achievable sum rate of SNR BIA is 1.36 times, 1.66 times, and 2.68 times that of data shared BIA, standard BIA, and extended BIA reported in the literature, respectively, and SNR BIA is more robust to user mobility.

INDEX TERMS Blind interference alignment, effective degree of freedom, SNR reduced factor, transmitter connection.

I. INTRODUCTION

The explosive growth of mobile traffic in the past decade requires advanced and practical solutions for improving both channel capacity and reliability, especially in wide area networks. Traditionally, channel resources are segmented into units, isolating each user's desired signal from the other users' signals to avoid their mutual interference. For example, in time division multiple access systems, one user exclusively occupies a certain number of slots at one frequency for its individual data transmission. With the fixed transmission capacity in each channel resource unit, the channel capacity is determined by the number of channel resource units, and the potential capacity improvement can be quite limited [1]. Recently, Interference Alignment (IA) [2]–[4] has been regarded as a promising technique to achieve the higher channel capacity. The basic idea of IA is to align one user's desired signal and the other users' signals (regarded as this user's interference) into the orthogonal spaces based on the Channel State Information (CSI). Thus they can be simultaneously transmitted in one channel unit. Then, each user recovers its own desired signal from the combination of its desired signal and interference.

The great performance improvement in IA is possible only under the assumption that the transmitter can perfectly obtain each user's CSI, which can be quite challenging to satisfy in practice. To address such problem, Blind Interference Alignment (BIA) [5]–[7] was developed from IA, and can achieve a high Degree of Freedom (DoF) without CSI at the transmitter. In BIA, the transmission scheme and receiving scheme are jointly designed. One user first receives its own desired signals together with the signals intended for other users and then independently receives the desired signal for every other user with the same channel state. Therefore, this user can subtract the interference (the desired signal for other users) from the signal combination and recover its own desired signal. Basically, BIA achieves capacity improvements without CSI through the agreement of transmission and receiving schemes for all users.

However, such tight coupling of the users' signal decoding hinders BIA from being extended to the large scale in both users and space. First, the current BIA mechanisms can achieve high channel capacity improvements under the infinite Signal-to-Noise Ratio (SNR) assumption [6]–[9]. Each user's desired signal decoding is related to the signals of other users and requires $K-1$ subtractions in the K-user BIA system, resulting in $K-1$ increases of noise accumulation [10], [11]. As the number of users K increases, each user's SNR declines significantly, inducing the deterioration of the transmission rate within each desired signal. Moreover, current BIA mechanisms generally design the transmission scheme and receiving. scheme for simple scenarios [12]–[14] (i.e., within one cell or the two transmitter toy model) but do not focus on the associated factors for BIA extension to multi-cell networks, such as which transmitter each user connects to and how each user joins the multi-cell BIA. More importantly, BIA extension to a large number of users and multi-cells are interactive with each other. In one cell with a fixed number of users, the noise accumulation can be alleviated by dividing users into groups based on their received SNRs, which is specified in our previous study [11]. In multi-cell networks, however, some users can connect to different transmitters, leading to different received SNRs and numbers of users in each cell, which further affects the overall performance of BIA.

There are several previous studies focusing on BIA in the two-cell network model. In [15], the authors applied interference coordination through data sharing to mitigate intercell interference for the cell edge users, while BIA was used to mitigate intracell interference. To improve the overall DoF, the authors in [16] assumed that two transmitters can share the data intended for the cell edge users and together send these data to the cell edge users. The location information was used in [17] to reduce the frame length in small cell networks and to eliminate both intracell interference and intercell interference. By assuming that the users in centers of the different cells are not interfering with each other, the authors in [18] regarded both cells' edge users as the private-users of one cell for intercell interference elimination. Different from these studies, in this paper, we consider the BIA design with finite received SNRs and focus on noise elimination in multi-cell networks. More specifically, this paper makes the following contributions:

1) Following our previously proposed user grouping scheme in a single cell [11], this paper theoretically analyzes the impact of transmitter connections on SNR deterioration in a two-cell network case.
2) A heuristic algorithm is proposed to jointly optimize the user grouping scheme and the transmitter connection in the multi-cell network, maximizing the overall DoF with limited SNR reduction.
3) Extensive simulations demonstrate that the achievable sum rate in SNR BIA is 1.36 times, 1.66 times, and 2.68 times the achievable sum rate of data shared BIA (dBIA) [16], standard BIA (sBIA) [6], and extended BIA (eBIA) [17], respectively, and that SNR BIA is also more robust to user mobility.

The paper is organized as follows. Section II presents the network model and motivation. Section III presents the user grouping scheme in one cell and analyzes the impact of transmitter connections on performances. Section IV proposes a heuristic algorithm for jointly optimizing user groupings and transmitter connections. Section V evaluates the performance of the multi-cell SNR BIA. Finally, Section VI concludes the paper.

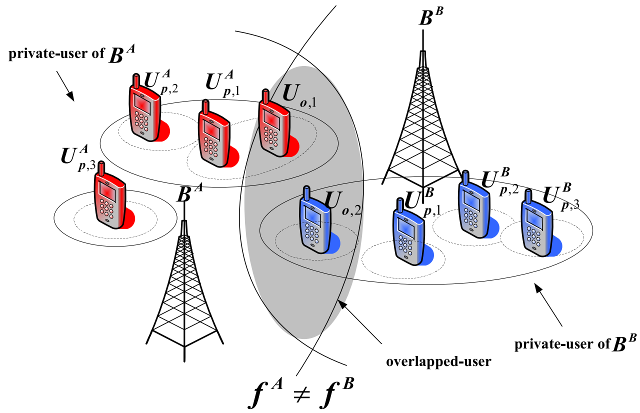

FIGURE 1. Network model.

II. NETWORK MODEL AND MOTIVATION

A. NETWORK MODEL

We consider the scenario where K users are distributed into a two-cell network, as shown in Fig. 1.[1] One transmitter (B^T, $T=A,B$) in each cell sends data to the users connected to it, and different transmitters work in different channels ($f_A \neq f_B$). Several users residing in only one cell can only connect to their corresponding transmitter. These users are regarded as *private-users* in this cell ($U^T_{p,i}$ in the white area in Fig. 1). The other users in the two cells' overlapping part can connect to more than one transmitter and are regarded as *overlapped-users* ($U_{o,i}$ in the shadow area in Fig. 1). Under the condition that B^T connects K^T_p private-users, and there are K_o total overlapped-users, the total number of users K can be expressed as

$$K = \sum_{T=A,B} K^T_p + K_o. \tag{1}$$

Assuming that $K^T_o, T = A, B$ overlapped-users connect to B^T, we have

$$\sum_{T=A,B} K^T_o = K_o. \tag{2}$$

Then, B^T's managed number of users K^T can be written as

$$K^T = K^T_p + K^T_o, \quad T = A, B. \tag{3}$$

[1]The model can be easily extended to a network with any number of cells. For simplicity, we take the two-cell scenario as the case for demonstration.

The Multiple Input Single Output (MISO) broadcast channel [15] is considered, in which the transmitter B^T has M antennas and each user has one reconfigurable antenna with M preset modes. B^T broadcasts the sum of the Encoded Data Streams (EDSs) intended for all the users connecting to it. The channels between the transmitter and the users are assumed to be block-fading channels [6]. That is, the channels remain static within one frame. Additionally, the channels between the transmitter and a single user in different modes are assumed to be independently and identically distributed (i.i.d.) [6].

In cell T, let U_i^T denote B^T's ith connected user. Then, the EDSs intended for U_i^T are defined as its *desired EDSs*, while the EDSs intended for the other user $U_j^T, j \neq i$, are defined as its *interference EDSs* (which are also the desired EDSs for U_j^T). When B^T broadcasts the sum of the desired EDSs to its managed users, U_i^T's received equation can be written as

$$y_i^T(t) = \mathbf{h}_i^T(q_i^T(t))(\mathbf{x}_i^T(t) + \sum_{U_i^T j \neq i} \mathbf{x}_j^T(t)) + z_i^T(t), \quad (4)$$

where $\mathbf{h}_i^T(\cdot)$ is a $1 \times M$-dimensional vector corresponding to M antennas. $\mathbf{h}_i^T(\cdot)$ denotes the channel between B^T and U_i^T. $q_i^T(t)$ denotes U_i^T's antenna mode in slot t. $\mathbf{x}_i^T(t)$ is an $M \times 1$-dimensional vector denotes the M desired EDSs for U_i^T sent by the transmitter's M antennas in slot t (one set of the desired EDSs for U_i^T). $\mathbf{x}_j^T(t)$ $(j \neq i)$ is one set of the desired EDSs for U_j^T, which is also one set of interference EDSs for U_i^T, and $z_i^T(t)$ is the complex white Gaussian noise, which and generally follows $\mathcal{CN}(0, 1)$ [6].

Each user U_i^T needs to eliminate its interference $\mathbf{x}_j^T(t)$, $\forall j \neq i$, to decode its own desired EDSs $\mathbf{x}_i^T(t)$. In BIA, such a goal is achieved by the transmitter B^T independently broadcasting $\mathbf{x}_j^T(t)$ in another slot t' and U_i^T receiving $\mathbf{x}_j^T(t)$ with the same antenna mode as that in t, i.e.,

$$y_i^T(t') = \mathbf{h}_i^T(q_i^T(t'))\mathbf{x}_j^T(t') + z_i^T(t'), \quad j \neq i, \quad (5)$$

where $q_i^T(t) = q_i^T(t')$, and $\mathbf{x}_j^T(t) = \mathbf{x}_j^T(t')$. Since slot t and slot t' are within the same frame and the channels between the transmitter and the users are block-fading, $\mathbf{h}_i^T(q_i(t)) = \mathbf{h}_i^T(q_i(t'))$. By subtracting (5) from (4), U_i^T can eliminate the interference EDSs $\mathbf{x}_j^T(t)$ in (4). In a similar way, U_i^T can eliminate each set of interference EDSs by independently receiving $\mathbf{x}_j^T(t)$ in another slot with the same antenna mode as that in t.

B. MOTIVATION

The interference elimination procedure described above will cause noise accumulation and SNR deterioration because $z_i^T(t)$ in (4) and $z_i^T(t')$ in (5) are generally i.i.d. and cannot be subtracted. Under the condition that there are K^T users connecting to B^T, it requires $K^T - 1$ subtractions for U_i^T to eliminate all the interference EDSs, increasing the noise power $K^T - 1$ fold. To evaluate such noise accumulation, we define *SNR reduced factor* s_i^T for each user U_i^T, to be the number of subtractions in its interference elimination procedure. Therefore, with the received SNR $rSNR_i^T$ of U_i^T, U_i^T's final Signal-to-Noise-Ratio (fSNR) after interference elimination is reduced by a factor of $s_i^T + 1$, i.e.,

$$fSNR_i^T = \frac{rSNR_i^T}{s_i^T + 1}. \quad (6)$$

Based on the above equation, fSNR depends on the following two factors: the user's SNR reduced factor and its rSNR. The SNR reduced factor is related to the number of users in its connected cell. The more users in the cell, the more interference EDSs this user needs to eliminate, and the higher the SNR reduced factor obtained by the user. The rSNR of the user is the received SNR related to its connected transmitter. In a multi-cell scenario, if a user is a private-user, its connected transmitter is fixed and its fSNR only depends on the SNR reduced factor in the cell in which it resides. If a user is an overlapped-user, it also has optional connected transmitters corresponding to different rSNRs. That is, its fSNR depends not only on its SNR reduced factor but also on the transmitter to which it connects.

fSNR is highly related to the transmission rate for each EDS. In fact, when fSNR is below a certain SNR threshold, i.e., SNR_{th}, the probability of decoding the desired EDSs can be greatly reduced, inducing capacity deterioration even though the DoF is increased [10]. To ensure that $fSNR \geq SNR_{th}$, we have proposed the constraint on the BIA mechanism [11] that s_i^T needs to be smaller than its maximum SNR reduced factor $\bar{s}_i^T$, i.e.,

$$s_i^T \leq \bar{s}_i^T, \quad \forall U_i^T, \forall T. \quad (7)$$

$\bar{s}_i^T$ can be calculated based on $rSNR_i^T$ and SNR_{th},

$$\bar{s}_i^T = \lfloor \frac{rSNR_i^T}{SNR_{th}} \rfloor - 1, \quad \forall U_i^T, \forall T. \quad (8)$$

When the fSNR of a user's desired EDSs is higher than SNR_{th}, the desired EDSs are considered to have been transmitted effectively, and the DoF corresponding to these desired EDSs is defined the as *effective DoF* (eDoF). Under the condition that a user's rSNR is not infinite, it is appropriate to use eDoF for evaluating performances. Our goal is to jointly determine to which transmitter each user connects and the BIA mechanism in each cell that maximizes the overall eDoF, i.e.,

$$\begin{aligned} &\max \ DoF \\ &s.t. \ s_i^T \leq \bar{s}_i^T, \quad \forall U_i^T, \forall T. \end{aligned} \quad (9)$$

III. USER GROUPING IN A TWO-CELL NETWORK

To reduce the negative impact of noise accumulation on performances, we proposed a user grouping based SNR BIA in [11]. The basic idea is to divide users into time-orthogonal groups, where each group further consists of several subgroups. The users in one subgroup receive their desired EDSs together and BIA is performed between different subgroups.

On the one hand, the number of subtractions for each user can be reduced, corresponding to a reduced SNR reduced factor. On the other hand, the users in different groups can have different SNR reduced factors adapting to their diverse rSNRs. We present the user grouping framework in a single cell in Section III. A and Section III. B. Then, we analyze the performance of the user grouping framework in the two-cell scenario in Section III. C. The notations used in this section are also summarized in Tab. 1.

TABLE 1. Summary of notations.

Notations	Descriptions
$U_{p,i}^{T}$	The ith private-user of B^T
$U_{o,i}$	The ith overlapped-user
U_i^T	The ith user connected to B^T
M_i^T	The number of transmitter's antenna sending desired EDSs for U_i^T
$\mathbf{x}_i^T$	One set of desired EDSs for U_i^T
$\mathbf{SB}_g^T$	The slot block for G_g^T
$\mathbf{X}_{g,s}^T$	One set of desired EDSs for the users in one subgroup $SG_{g,s}^T$
$\mathbf{X}_{g,s}^{T,i}$	The ith set of desired EDSs for the users in one subgroup $SG_{g,s}^T$
$\mathbf{T}_{g,O}^T(n)$	The nth step of the transmission scheme in the overlapped part in $\mathbf{SB}_g^T$
$\mathbf{T}_{g,O}^{T,i}(n)$	The ith set of $\mathbf{T}_{g,O}^T(n)$
$\mathbf{Q}_{g,O}^T(n)$	The nth step of the receiving scheme in the overlapped part in $\mathbf{SB}_g^T$

We first present the user grouping framework. The users in each cell T are divided into groups. One group G_g^T, $\forall g, \forall T$ contains $n_{g,p}^T$ private-users and $n_{g,o}^T$ overlapped-users. Within G_g^T, the users further form several subgroups, with each subgroup $SG_{g,s}^T$ including $n_{g,s,p}^T$ private-users and $n_{g,s,o}^T$ overlapped-users. Let $|G^T|$ be the number of groups and let $|G_g^T|$ be the number of subgroups of G_g^T. Then,

$$\sum_{g=1}^{|G^T|}\sum_{s=1}^{|G_g^T|}(n_{g,s,p}^T + n_{g,s,o}^T) = K_p^T + K_o^T, \quad \forall T. \tag{10}$$

For example, as shown in Fig. 1, three private-users of B^A ($U_{p,i}^A$, $i = 1, 2, 3$) and one overlapped-user $U_{o,1}$ connect to B^A, while three private-users of B^B ($U_{p,i}^B$, $i = 1, 2, 3$) and one overlapped-user $U_{o,2}$ connect to B^B. In cell B^A, the connected users form two groups (two solid-line circles) with three users in G_1^A and one user in G_2^A. G_1^A further consists of two subgroups (two dashed-line circles). The users connecting to B^B form one group, in which each user forms one subgroup.

B^T transmits desired EDSs for G_g^T's different subgroups within a fraction of the exclusive slots ($\mathbf{SB}_g^T$). $\mathbf{X}_{g,s}^T$, an $M \times 1$-dimensional vector, denotes one set of desired EDSs intended for the users in $SG_{g,s}^T$. $\mathbf{x}_i^T$, an $M_i^T \times 1$-dimensional vector, denotes U_i^T's desired EDSs (B^T transmits M_i^T desired EDSs to $U_i^T \in SG_{g,s}^T$). Then,

$$\sum_{U_i^T \in SG_{g,s}^T} M_i^T = M, \quad \forall g, s, T. \tag{11}$$

$$\mathbf{X}_{g,s}^T = \left[\cdots \mathbf{x}_i^{T\dagger} \cdots \mathbf{x}_j^{T\dagger} \cdots\right]^\dagger, \quad \forall g, s, T; \quad U_i^T, U_j^T \in SG_{g,s}^T, \tag{12}$$

where $\mathbf{x}_i^{T\dagger}$ denotes the transpose of $\mathbf{x}_i^T$. Since $U_i^T \in SG_{g,s}^T$ needs to receive at least one desired EDS, the number of users in each subgroup satisfies

$$n_{g,s,p}^T + n_{g,s,o}^T \in [1, M]. \tag{13}$$

Each user in a subgroup needs to decode all the desired EDSs for its subgroup to obtain its own desired EDSs. For example, U_i^T needs to decode $\mathbf{X}_{g,s}^T$ for its own desired EDSs $\mathbf{x}_i^T$. Based on this design, BIA can be performed between different subgroups within a certain group. That is, $U_i^T \in SG_{g,s}^T$ receives both its subgroup desired EDSs $\mathbf{X}_{g,s}^T$ and its subgroup interference EDSs $\mathbf{X}_{g,u}^T$, $\forall u \neq s$. Its received equation is

$$\begin{aligned} y_i^T(t) &= \mathbf{h}_i^T(q_i^T(t)) \\ &\times [\underbrace{\mathbf{X}_{g,s}^T(t)}_{\text{desired EDSs for } SG_{g,s}^T} + \underbrace{\sum_{u\neq s}\mathbf{X}_{g,u}^T(t)}_{\text{subgroup interference EDSs for } SG_{g,s}^T}] \\ &+ z_i^T(t), \quad \forall U_i^T \in SG_{g,s}^T. \end{aligned} \tag{14}$$

The purpose of SNR BIA is to design the transmission scheme and receiving scheme, so that each user can eliminate its subgroup interference EDSs. SNR BIA can be designed in the following two parts: overlapped part and independent part. In the overlapped part, the desired EDSs for all the subgroups in G_g^T are transmitted simultaneously. In the independent part, the desired EDSs for each subgroup are independently transmitted.

A. SIMPLE CASE OF THE TRANSMISSION SCHEME AND RECEIVING SCHEME

We consider cell A in Fig. 1 as a simple case, in which B^A has two antennas ($M = 2$) and one overlapped-user $U_{o,1}$ connects to B^A. Cell A includes two groups ($G_1^A = \{U_{p,1}^A, U_{p,2}^A, U_{o,1}\}$ and $G_2^A = \{U_{p,3}^A\}$), and G_1^A further consists of two subgroups ($SG_{1,1}^A = \{U_{p,1}^A, U_{o,1}\}$ and $SG_{1,2}^A = \{U_{p,2}^A\}$). $U_{p,1}^A$ and $U_{o,1}$ are each sent one desired EDS in $SG_{1,1}^A$. Therefore,

$$\begin{aligned} \mathbf{X}_{1,1}^A &= [\mathbf{x}_{p,1}^{A\dagger}, \mathbf{x}_{o,1}^{A\dagger}]^\dagger. \\ \mathbf{X}_{1,2}^A &= \mathbf{x}_{p,2}^A. \\ \mathbf{X}_{2,1}^A &= \mathbf{x}_{p,3}^A. \end{aligned} \tag{15}$$

The transmission scheme and receiving scheme are illustrated in Fig. 2. G_1^A and G_2^A occupy 3 slots and 2 slots, respectively. For G_1^A, B^A broadcasts the sum of the desired

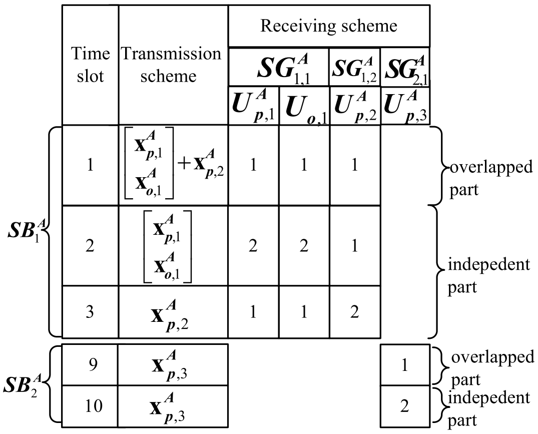

FIGURE 2. The transmission scheme and receiving scheme of cell A ($M = 2$) in Fig. 1.

EDSs for all of G_1^A's subgroups in the 1st slot (overlapped part), and then independently broadcasts the desired EDS for each subgroup (independent part). Correspondingly, each user receives the specific interference EDS with the same antenna mode, but receives its desired EDSs with different modes. Specifically, $U_{p,1}^A$ receives its interference EDSs $\mathbf{X}_{1,2}^A = \mathbf{x}_{p,2}^A$ with mode 1 in both slot 1 and slot 3, while receiving its desired EDSs $\mathbf{X}_{1,1}^A = [\mathbf{x}_{p,1}^{A\ \dagger}, \mathbf{x}_{o,1}^{A\ \dagger}]^\dagger$ with mode 1 and mode 2 in slot 1 and slot 2, respectively. The received equations of $U_{p,1}^A$ are

$$\begin{bmatrix} y_{p,1}^A(1) \\ y_{p,1}^A(2) \\ y_{p,1}^A(3) \end{bmatrix} = \begin{bmatrix} \mathbf{h}_{p,1}^A(1) \\ \mathbf{h}_{p,1}^A(2) \\ \mathbf{0} \end{bmatrix} \begin{bmatrix} \mathbf{x}_{p,1}^A \\ \mathbf{x}_{o,1}^A \end{bmatrix} + \begin{bmatrix} \mathbf{h}_{p,1}^A(1) \\ \mathbf{0} \\ \mathbf{h}_{p,1}^A(1) \end{bmatrix} \mathbf{x}_{p,2}^A + \begin{bmatrix} z_{p,1}^A(1) \\ z_{p,1}^A(2) \\ z_{p,1}^A(3) \end{bmatrix}. \tag{16}$$

$\mathbf{x}_{p,2}^A$ can be eliminated by subtracting $y_{p,1}^A(3)$ from $y_{p,1}^A(1)$, i.e.,

$$\begin{bmatrix} y_{p,1}^A(1) - y_{p,1}^A(3) \\ y_{p,1}^A(2) \end{bmatrix} = \begin{bmatrix} \mathbf{h}_{p,1}^A(1) \\ \mathbf{h}_{p,1}^A(2) \end{bmatrix} \begin{bmatrix} \mathbf{x}_{p,1}^A \\ \mathbf{x}_{o,1}^A \end{bmatrix} + \begin{bmatrix} z_{p,1}^A(1) - z_{p,1}^A(3) \\ z_{p,1}^A(2) \end{bmatrix}. \tag{17}$$

There are two independent received equations in (17). $U_{p,1}^A$ can decode two variables $\mathbf{x}_{p,1}^A$ and $\mathbf{x}_{o,1}^T$, where $\mathbf{x}_{p,1}^A$ is its desired EDS. Similarly, other users in G_1^A can decode their desired EDSs. In G_2^A, $U_{p,3}^A$ independently forms one group without interference, and can decode its desired EDSs.

Two observations can be obtained from the above example. First, the users in a subgroup receive their desired EDSs together, and they also receive the interference caused by the users in the same subgroup. Hence the interference caused by the users in the same subgroup can be eliminated together, so that the users will have the smaller SNR reduced factor than that they would have had in the BIA without the user grouping framework. Second, the users in different groups have different SNR reduced factors. For example, $s_{p,1}^A = 1$, $s_{p,2}^A = 1$, $s_{o,1}^A = 1$, and $s_{p,3}^A = 0$. However, in the standard BIA [6], each user's SNR reduced factor is 3. This difference is a result of the allocation of users into different groups with different subgroups.

B. GENERAL CASE OF THE TRANSMISSION SCHEME AND RECEIVING SCHEME

Because the slot blocks for different groups are time-orthogonal, different groups follow the same transmission scheme and receiving scheme design, and without loss of generality, we focus on a certain group G_g^T. The slot block for G_g^T is still divided into the following two parts: the overlapped part and the independent part. To present the scheme intuitively, a complicated example is analyzed.[2]

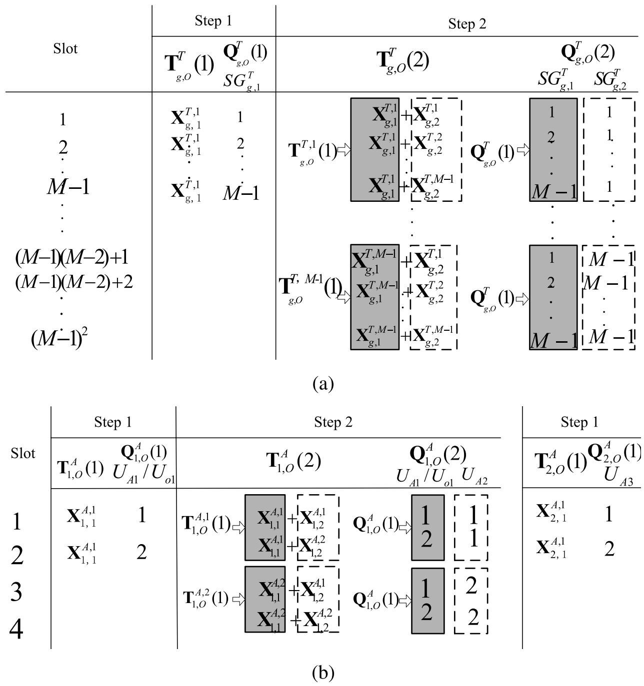

FIGURE 3. The first two steps of the transmission scheme and receiving scheme in the overlapped part of SB_g^T. (a) The general case. (b) The example of cell A ($M = 3$) in Fig. 1.

1) OVERLAPPED PART

The transmission scheme $\mathbf{T}_{g,O}^T$ and receiving scheme $\mathbf{Q}_{g,O}^T$ in the overlapped part are constructed in an iterative way. In the first step, $\mathbf{T}_{g,O}^T(1)$ and $\mathbf{Q}_{g,O}^T(1)$ are designed as shown in Fig. 3 (a). $\mathbf{T}_{g,O}^T(1)$ is constructed by $\mathbf{X}_{g,1}^{T,1}$ ($SG_{g,1}^T$'s 1st set of desired EDSs) transmitting $M-1$ times. Correspondingly, each user in $SG_{g,1}^T$ configures its antenna from mode 1 to

[2]We still consider the example in the previous subsection. The difference is that B^A has $M = 3$ antennas, and $U_{p,1}^A$ is sent 2 desired EDSs and $U_{o,1}^A$ is sent one desired EDS in $SG_{1,1}^A$.

mode $M-1$, constructing $\mathbf{Q}_{g,O}^{T}(1)$. $\mathbf{T}_{g,O}^{T}(1)$ ($\mathbf{Q}_{g,O}^{T}(1)$) occupies $l_{g,O}^{T}(1)=M-1$ slots, constructing $M-1$ independent received equations (the Mth independent received equation is contributed in the independent part). For the example, $\mathbf{T}_{1,O}^{A}(1)$ ($\mathbf{Q}_{1,O}^{A}(1)$) and $\mathbf{T}_{2,O}^{A}(1)$ ($\mathbf{Q}_{2,O}^{A}(1)$) are designed as shown in Fig. 3 (b).[3]

$\mathbf{T}_{g,O}^{T}(2)$ and $\mathbf{Q}_{g,O}^{T}(2)$ are designed based on $\mathbf{T}_{g,O}^{T}(1)$ and $\mathbf{Q}_{g,O}^{T}(1)$, respectively. First, $\mathbf{T}_{g,O}^{T}(1)$ is repeated $M-1$ times, forming $M-1$ grey boxes in $\mathbf{T}_{g,O}^{T}(2)$. The transmission scheme in the ith grey box $\mathbf{T}_{g,O}^{T,i}(1)$ is the same as that in $\mathbf{T}_{g,O}^{T}(1)$, but for different sets of EDSs. After that, $M-1$ sets of the desired EDSs for $SG_{g,2}^{T}$ ($\mathbf{X}_{g,2}^{T,i}, i=1,\ldots,M-1$) are transmitted once, forming one dashed-line box, and this is further repeated $M-1$ times. As for the example in Fig. 3 (b), $\mathbf{T}_{1,O}^{A,1}(2)$ and $\mathbf{T}_{1,O}^{A,2}(2)$ have the same transmission scheme, but $\mathbf{T}_{1,O}^{A,2}(2)$ contains different sets of desired EDSs from $\mathbf{T}_{1,O}^{A,1}(2)$ (that is, $\mathbf{X}_{1,1}^{A,1}$ and $\mathbf{X}_{1,1}^{A,2}$ are different sets of desired EDSs for $SG_{1,1}^{A}$). Then, $\mathbf{X}_{1,2}^{A,j}$, $j=1,2$ are added into one dashed-line box, and are repeated $M-1=2$ times. Second, $\mathbf{Q}_{g,O}^{T}(1)$ is repeated $M-1$ times forming $M-1$ grey boxes in $\mathbf{Q}_{g,O}^{T}(2)$. The users in the newly added subgroup $SG_{g,2}^{T}$ configure their antenna modes from mode 1 to mode $M-1$, each mode forming one dashed-line box, and this is further repeated $M-1$ times. $\mathbf{T}_{g,O}^{T}(2)$ ($\mathbf{Q}_{g,O}^{T}(2)$) occupies $l_{g,O}^{T}(2)=(M-1)^2$ slots. Corresponding to the example in Fig. 3 (b), $\mathbf{Q}_{1,O}^{A}(1)$ is repeated $M-1=2$ times, forming two grey boxes. $U_{p,2}^{A}\in SG_{1,2}^{A}$ configures its antennas to mode 1, forming the first dashed-line box, and to mode 2, forming the second dashed-line box.[4]

Such a design ensures that the users in both $SG_{g,1}^{T}$ and $SG_{g,2}^{T}$ receive their desired EDSs with different modes, and receive their interference EDSs with the same mode. For example, in Fig. 3 (b), the users in $SG_{1,1}^{A}$ receive their desired EDSs ($\mathbf{X}_{1,1}^{A,i}, i=1,2$) in two different modes, and receive their interference EDSs ($\mathbf{X}_{1,2}^{A,i}, i=1,2$) in the same mode. Additionally, $U_{p,3}^{A}\in SG_{1,2}^{A}$ receives $\mathbf{X}_{1,2}^{A,i}, i=1,2$ in two different modes, and receives $\mathbf{X}_{1,1}^{A,i}, i=1,2$ in the same mode.

Generally, assuming that $\mathbf{T}_{g,O}^{T}(n-1)$ is designed for the first $n-1$ subgroups ($n\le|G_g^T|$) as shown in the grey box in Fig. 4 (a), $\mathbf{T}_{g,O}^{T}(n)$ can be designed based on $\mathbf{T}_{g,O}^{T}(n-1)$ as follows:

- $\mathbf{T}_{g,O}^{T}(n-1)$ is repeated $M-1$ times, forming $M-1$ grey boxes. The transmission schemes of different grey boxes are the same, but for different sets of desired EDSs.
- $(M-1)^{n-1}$ sets of desired EDSs for the nth subgroup are added, forming one dashed-line box, and this is further repeated $M-1$ times.

[3]Since $|G_2^A|=1$, the overlapped part of the design of $\mathbf{SB}_2^A$ has been finished.

[4]Since $|G_1^A|=2$, the overlapped part design of $\mathbf{SB}_1^A$ has been finished.

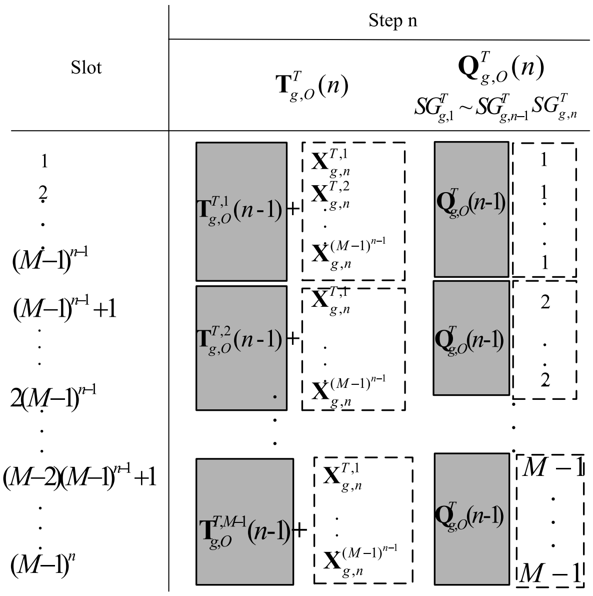

FIGURE 4. The nth step of the transmission scheme and receiving scheme in the overlapped part of $\mathbf{SB}_g^T$.

Correspondingly, $\mathbf{Q}_{g,O}^{T}(n)$ is designed based on $\mathbf{Q}_{g,O}^{T}(n-1)$ as follows.

- $\mathbf{Q}_{g,O}^{T}(n-1)$ is repeated $M-1$ times, forming $M-1$ grey boxes for the users in $SG_{g,s}^{T}$, $s=1,\ldots,n-1$.
- For the users in $SG_{g,n}^{T}$, their antennas are configured to mode i within the ith dashed-line box, $i=1,\ldots,M-1$.

After the nth step, the overlapped part in $\mathbf{SB}_g^T$ includes $(M-1)^n$ slots for n subgroups. Since G_g^T contains $|G_g^T|$ subgroups, the total number of slots in the overlapped part of $\mathbf{SB}_g^T$ is

$$l_{g,O}^{T}=(M-1)^{|G_g^T|}. \tag{18}$$

Each set of desired EDSs for one subgroup is transmitted $M-1$ times, occupying $M-1$ slots in the overlapped part. Hence

$$ES_{g,s}^{T}=l_{g,O}^{T}/(M-1)=(M-1)^{|G_g^T|-1} \tag{19}$$

sets of desired EDSs are transmitted for $SG_{g,s}^{T}$ in $\mathbf{SB}_g^T$.

2) INDEPENDENT PART

To eliminate the interference EDSs for each user and construct the Mth independent equation for decoding the desired EDSs, each set of EDSs also needs to be independently transmitted once. For the slot where $\mathbf{X}_{g,s}^{T,j}$, $\forall j$ is transmitted, if $U_i^T\in SG_{g,s}^{T}$, then U_i^T receives its subgroup's desired EDSs with mode M. If $U_i^T\notin SG_{g,s}^{T}$, to subtract the interference EDSs in the overlapped part, U_i^T needs to receive $\mathbf{X}_{g,s}^{T,j}$ in the same antenna mode as those in the overlapped part. In the $M=3$ case mentioned before, the independent part is designed as shown in Fig. 5. Taking $U_{p,1}^{A}$ as an example, it receives the interference EDSs $\mathbf{X}_{1,2}^{A,1}=\mathbf{x}_{p,2}^{A,1}$ in the 1st slot and the 3rd slot (in the overlapped part) with mode 1, and

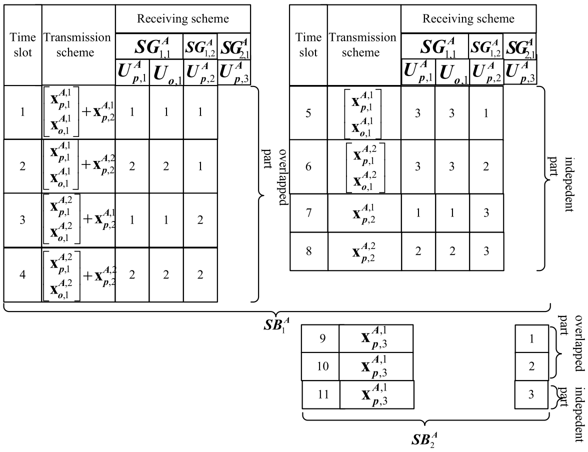

FIGURE 5. The transmission scheme and receiving scheme of the example with $M = 3$.

independently receives $\mathbf{X}_{1,2}^{A,1} = \mathbf{x}_{p,2}^{A,1}$ in the 7th slot (in the independent part) with mode 1. Meanwhile, $U_{p,1}^{A}$ receives its subgroup desired EDSs $\mathbf{X}_{1,1}^{A,1} = [\mathbf{x}_{p,1}^{A,1\dagger}, \mathbf{x}_{o,1}^{A,1\dagger}]^{\dagger}$ in the 5th slot (in the independent part) with mode 3.

Since $ES_{g,s}^{T}$ sets of desired EDSs (based on (19)) are transmitted to $SG_{g,s}^{T}$, $s = 1, \ldots, |G_g^T|$ and each set occupies one slot in the independent part, the number of slots in the independent part is

$$l_{g,I}^{T} = \sum_{g=1}^{|G_g^T|} ES_{g,s}^{T} = |G_g^T|(M-1)^{|G_g^T|-1}. \tag{20}$$

C. PERFORMANCE ANALYSIS FOR USER GROUPING IN A TWO-CELL NETWORK

$U_i^T \in SG_{g,s}^T$ requires $|G_g^T| - 1$ subtractions to eliminate the $|G_g^T|-1$ sets of interference in the overlapped part. Therefore, U_i^T's SNR reduced factor is

$$s_i^T = |G_g^T| - 1, \quad \forall U_i^T \in G_g^T,\ T = A, B. \tag{21}$$

It can be observed that s_i^T is uniquely determined by the number of subgroups in the group to which U_i^T belongs. Then, the SNR reduced factor constraint in (7) is equivalent to

$$|G_g^T| \le \bar{s}_i^T + 1, \quad \forall U_i^T \in G_g^T,\ T = A, B. \tag{22}$$

In addition, the user grouping scheme also needs to follow the restrictions given as equations (2), (10), and (13). Then, the problem in a two-cell network can be formulated as

$$\begin{aligned} &\max\ DoF \\ &s.t.\ |G_g^T| \le \bar{s}_i^T + 1, \quad \forall g, T = A, B;\ \forall U_i^T \in G_g^T, \\ &\quad n_{g,s,p}^T + n_{g,s,o}^T \in [1, M], \quad \forall g, s, T = A, B, \\ &\quad \sum_{g=1}^{|G^T|}\sum_{s=1}^{|G_g^T|}(n_{g,s,p}^T + n_{g,s,o}^T) = K_p^T + K_o^T, \\ &\quad K_o^A + K_o^B = K_o. \end{aligned} \tag{23}$$

Theorem 1: The DoF of a two-cell SNR BIA is

$$\begin{aligned} &DoF_{\text{SNR BIA}} \\ &= \frac{1}{2}\sum_{T=A,B}\frac{\sum_{g=1}^{|G^T|}(M|G_g^T|(M-1)^{|G_g^T|-1})}{\sum_{g=1}^{|G^T|}(|G_g^T|M-1)^{|G_g^T|-1} + (M-1)^{|G_g^T|})}, \end{aligned} \tag{24}$$

where the users connected to B^T are divided into $|G^T|$ groups and the group G_g^T contains $|G_g^T|$ subgroups.

Proof: Based on (19), $(M-1)^{|G_g^T|-1}$ sets of EDSs are transmitted, intended for the users in one subgroup $SG_{g,s}^T$, each containing M EDSs. Then, the number of EDSs transmitted to G_g^T (including $|G_g^T|$ subgroups) is

$$E_g^T = M|G_g^T|(M-1)^{|G_g^T|-1}, \quad \forall g;\ T = A, B. \tag{25}$$

Based on (18) and (20), the number of slots in $\mathbf{SB}_g^T$ is

$$\begin{aligned} l_g^T = l_{g,O}^T + l_{g,I}^T = (M-1)^{|G_g^T|} + |G_g^T|(M-1)^{|G_g^T|-1}, \\ \forall g;\quad T = A, B. \end{aligned} \tag{26}$$

$|G^T|$ time-orthogonal groups are contained in B^T, and the DoF of cell B^T is

$$DoF_{\text{SNR BIA}}^T = \frac{\sum_{g=1}^{|G^T|} E_g^T}{\sum_{g=1}^{|G^T|} l_g^T};\quad T = A, B. \tag{27}$$

Since the transmitters in the two cells send EDSs at two different frequencies, the overall DoF of the two-cell network is

$$\begin{aligned} &DoF_{\text{SNR BIA}} \\ &= \sum_{T=A,B}\frac{1}{2}DoF_{\text{SNR BIA}}^T \\ &= \frac{1}{2}\sum_{T=A,B}\frac{\sum_{g=1}^{|G^T|}(M|G_g^T|(M-1)^{|G_g^T|-1})}{\sum_{g=1}^{|G^T|}(|G_g^T|M-1)^{|G_g^T|-1} + (M-1)^{|G_g^T|})}. \end{aligned} \tag{28}$$

Based on Theorem 1, $DoF_{\text{SNR BIA}}$ is only related to the number of subgroups in each group. Therefore, once the number of subgroups in each group has been determined, the allocation of the users into subgroups does not affect $DoF_{\text{SNR BIA}}$.

Proposition 1: To achieve the maximum DoF in G_g^T based on the user grouping-scheme, the number of subgroups is

$$|G_g^T| = \min(\sum_{s=1}^{|G_g^T|}(n_{g,s,p}^T + n_{g,s,o}^T),\ \min_{U_i^T \in G_g^T}(\overline{s_i^T}) + 1) \tag{29}$$

with the restriction

$$\sum_{s=1}^{|G_g^T|}(n_{g,s,p}^T + n_{g,s,o}^T) \leq M|G_g^T|. \tag{30}$$

Proof: Based on the first constraint in (23), $|G_g^T|$ needs to be smaller than $\overline{s_i^T} + 1, \forall U_i^T \in G_g^T$, i.e.,

$$|G_g^T| \leq \min_{U_i^T \in G_g^T} (\overline{s_i^T}) + 1. \tag{31}$$

In addition, based on the second constraint in (23),

$$|G_g^T| \leq \sum_{s=1}^{|G_g^T|}(n_{g,s,p}^T + n_{g,s,o}^T) \leq M|G_g^T|. \tag{32}$$

Combining (31) and (32), the feasible number of subgroups $|G_g^T|$ needs to satisfy

$$|G_g^T| \leq \min(\sum_{s=1}^{|G_g^T|}(n_{g,s,p}^T + n_{g,s,o}^T), \quad \min_{U_i \in G_g^T} (\overline{s_i^T}) + 1). \tag{33}$$

Based on Theorem 1, a larger number of subgroups leads to a larger DoF. Hence the number of subgroups for maximizing the DoF in G_g^T is

$$|G_g^T| = \min(\sum_{s=1}^{|G_g^T|}(n_{g,s,p}^T + n_{g,s,o}^T), \quad \min_{U_i^T \in G_g^T} (\overline{s_i^T}) + 1). \tag{34}$$

Additionally, in (32), the number of users in G_g^T should satisfy

$$\sum_{s=1}^{|G_g^T|}(n_{g,s,p}^T + n_{g,s,o}^T) \leq M|G_g^T|, \quad \forall g; \; T = A, B. \tag{35}$$

Proposition 1 is proved.

IV. JOINT OPTIMIZATION OF USER GROUPING AND TRANSMITTER CONNECTION

In the two-cell network, an overlapped-user's transmitter connection will affect both the number of users in one cell and this user's maximum SNR reduced factor.[5] These two factors further affect the transmission scheme and receiving scheme of the user grouping scheme. In this section, the user grouping and the transmitter connections are jointly optimized for maximizing the optimization objective in (28).

[5] The transmitter accumulates each user's maximum SNR reduced factor for determining the transmitter connection and user grouping scheme. Specifically, the transmitters can first broadcast the pilots in the beginning of the frame. Then, the users feedback their rSNRs to the transmitter. Based on (8), with a certain SNR threshold, the transmitter can calculate the maximum SNR reduced factor for the users.

A. IMPACT OF TRANSMITTER CONNECTION ON USER GROUPING SCHEME

We demonstrate the impact of transmitter connection on performances through an example, as shown in Fig. 1. B^A and B^B each have three antennas ($M = 3$). We assume that B^A has three private-users $U_{p,1}^A$, $U_{p,2}^A$, and $U_{p,3}^A$, with the maximum SNR reduced factors $\overline{s}_{p,1}^A = \overline{s}_{p,2}^A = 2$ and $\overline{s}_{p,3}^A = 0$. Based on the first constraint in (23), there are at most $\overline{s}_{p,1}^A + 1 = 3$ ($\overline{s}_{p,2}^A + 1 = 3$) subgroups in the group in which $U_{p,1}^A$ ($U_{p,2}^A$) resides. Since $U_{p,3}^A$'s SNR reduced factor is 0, it can only independently form one group to ensure that its fSNR is greater than SNR_{th} ($\overline{s}_{p,3}^A + 1 = 1$). B^B has three private-users, $U_{p,1}^B$, $U_{p,2}^B$, and $U_{p,3}^B$, with the maximum SNR reduced factors $\overline{s}_{p,i}^B = 3$, $i = 1, 2, 3$. Therefore, $U_{p,i}^B$, $i = 1, 2, 3$, can reside in the group with at most $\overline{s}_{p,i}^B + 1 = 4$ subgroups. Two overlapped-users $U_{o,1}$ and $U_{o,2}$ are within the overlapped area. $U_{o,1}$'s maximum SNR reduced factors connecting B^A and B^B are $\overline{s}_{o,1}^A = 1$ and $\overline{s}_{o,1}^B = 2$, respectively. $U_{o,2}$'s maximum SNR reduced factors connecting B^A and B^B are $\overline{s}_{o,1}^A = 1$ and $\overline{s}_{o,1}^B = 3$, respectively. The above scenario is also presented in the left part in Fig. 6.

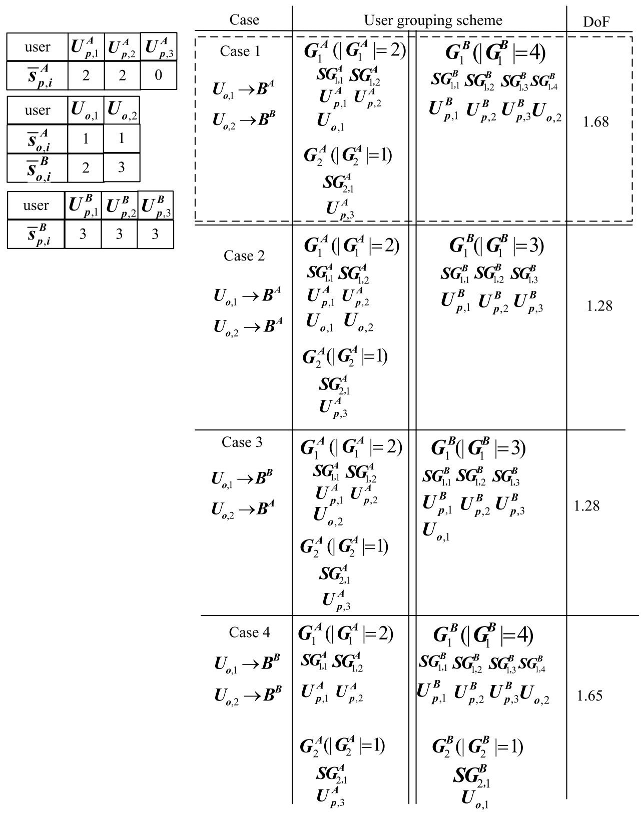

FIGURE 6. User grouping scheme and transmitter connection cases for the model shown in Fig. 1.

We list all the transmitter connection cases and compare their impacts on DoF. For a specific transmitter connection case, the optimal user grouping scheme in (23) is selected.[6] For example, in Case 1, $U_{o,1}$ connects to the transmitter B^A and $U_{o,2}$ connects to the transmitter B_A. In this case, the users connecting to B^A form the following two groups ($|G_1^A| = 2$): $U_{p,1}^A$, $U_{p,2}^A$ and $U_{o,1}$ form G_1^A, and $U_{p,3}$ independently forms G_2^A. G_1^A consists of the following two subgroups $SG_{1,1}^A = \{U_{p,1}^A, U_{o,1}\}$ and $SG_{1,2}^A = \{U_{p,2}^A\}$. This user grouping choice satisfies the constraints in (23) and achieves the maximum overall DoF for B^A. In addition, B^B's private-users form one group, $G_1^B = \{U_{p,1}^B, U_{p,2}^B, U_{p,3}^B, U_{o,2}\}$. Based on (30), $|G_1^B| = 4$. Therefore, each user forms one subgroup. This achieves the maximum DoF for B^B. Similarly, we also present the user grouping results (Cases 2-4) for the other transmitter connection cases.

First, different transmitter connection cases can result in different numbers of users in each of the two cells, which affects the overall DoF. In Case 1, $U_{o,1}$ connects to B^A ($\bar{s}_{o,1}^A = 1$) and $U_{o,2}$ connects to B^B ($\bar{s}_{o,1}^B = 3$). To maximize the overall DoF, based on (30), $U_{p,1}^B$, $U_{p,2}^B$, $U_{p,3}^B$, and $U_{o,2}$ form one group, and within the group, each forms one subgroup. $U_{p,1}^A$, $U_{p,2}^A$ and $U_{p,3}^A$ form one group with two subgroups ($SG_{1,1}^A = \{U_{p,1}^A, U_{o,1}\}$ and $SG_{1,2}^A = \{U_{p,2}^A\}$) and $U_{p,3}^A$ alone forms one group. Based on (27), the overall DoF is 1.68. In Case 2, however, all overlapped-users connect to B^A and there are no overlapped-users connecting to B^B. The three private-users connecting to B^B can only form one group with three subgroups based on (30). Meanwhile, in the cell A, to maximize the DoF, $U_{p,1}^A$, $U_{p,2}^A$, $U_{o,1}$, and $U_{o,2}$ form G_1^A with two subgroups $SG_{1,1}^A = \{U_{p,1}^A, U_{o,1}\}$ and $SG_{1,2}^A = \{U_{p,2}^A, U_{o,1}\}$. $U_{p,3}^A$ forms one group $G_2^A = \{U_{p,3}^A\}$. Based on (27), the overall DoF is 1.28. The difference in the performances of Case 1 and Case 2 is the result of the different numbers of subgroups in each group. Based on Theorem 1, the DoF in a group is determined by the number of subgroups in this group. The larger the number of subgroups a group includes, the larger the DoF that this group can achieve. Because there are three subgroups in cell B in Case 2, which is smaller than in Case 1, the DoF achieved in cell B in Case 2 is smaller than that in Case 1. Additionally, adding $U_{o,2}$ to B^A does not increase the number of subgroups of G_1^A, but only results in dispersed EDS allocations. Therefore, the DoF achieved in cell A in Case 2 is the same as that in Case 1.

The transmitter connection affects the overall performances through different rSNRs in Case 1 and Case 3. Specifically, in both Case 1 and Case 3, one overlapped-user connects to B^A and the other connects to B^B. In Case 3, however, since $U_{o,1}$ connects to B_B ($\bar{s}_{o,1}^B = 2$), to satisfy the first constraint in (23) ($|G_1^B| \le \bar{s}_i^B + 1, \forall U_i^B \in G_1^B$), $|G_1^B|$ can be at most 3. Meanwhile, in cell A, to maximize the DoF, $U_{p,1}^A$, $U_{p,2}^A$, $U_{o,1}$, and $U_{o,2}$ form G_1^A with two subgroups $SG_{1,1}^A = \{U_{p,1}^A, U_{o,1}\}$ and $SG_{1,2}^A = \{U_{p,2}^A, U_{o,1}\}$. $U_{p,3}^A$ forms one group, $G_2^A = \{U_{p,3}^A\}$. Therefore, based on (27), the overall DoF is 1.28. The difference in the performances of Case 1 and Case 3 is the result of the difference in rSNRs when overlapped users connect different transmitters. In Case 3, there are three users ($U_{p,i}^B, i = 1, 2, 3$) with the maximum SNR reduced factor 3, and one user ($U_{o,2}^B$) with the maximum SNR reduced factor 2 in cell B. Hence, the number of subgroups in G_1^B can be only 3, which is smaller than that (4 subgroups) in Case 1.

From the above analysis, the transmitter connection will affect the following two factors: the number of users in the cell and the overlapped-users' rSNRs. These two factors result in the different DoFs. Therefore in a multi-cell network, these two factors need to be jointly considered for optimizing the overall DoF.

B. JOINT OPTIMIZATION OF TRANSMITTER CONNECTION AND USER GROUPING

The problem in (23) can be easily verified to be an a NP-complete problem, and we propose a heuristic algorithm to optimize it in this section. The optimization objective in (23) is related to both transmitter connection and user grouping scheme. Once a group's number of users is given, the DoF in this group is only correlated with the number of subgroups, based on Theorem 1. Therefore, the basic idea is to jointly adjust the transmitter connection and the user grouping scheme, so that the users in this group can achieve as the large DoF as possible with the restrictions in (23) satisfied. To better illustrate the algorithm, the joint optimization of the example in Section IV (Fig. 6) is presented.

Specifically, the algorithm consists of a certain number of rounds, and each round forms one group through the following three steps.

1) STEP 1 (FORMING THE UNGROUPED USER TABLE)

The users (including the private-users in each cell and all overlapped-users) who are not allocated into the group are regarded as ungrouped users. All ungrouped users in the tth round and their maximum SNR reduced factors are listed in an *ungrouped user table*, where each item includes one ungrouped user and the maximum SNR reduced factors for its potential connected transmitters. In the two-cell network, each private-user has only one maximum SNR reduced factor, and each overlapped-user can have two different maximum SNR reduced factors corresponding to different transmitters. The ungrouped user table for the example in Section IV is shown in the left part in Fig. 7. $U_{o,1}$ and $U_{o,2}$ have different maximum SNR reduced factors for B^A and B^B.

2) STEP 2 (FORMING THE GROUP)

Step 2.1 (Select the First User in the Group and Its Connected Transmitter): Within the ungrouped user table, we select the user with the maximum SNR reduced factor, and its corresponding connected transmitter B^T is the

[6] In this example, we can exhaustively search all possible user grouping choices to find the maximum overall DoF. For the more complicated examples, it can be proved that this is an NP-complete problem, and a heuristic algorithm is proposed in Section IV.B.

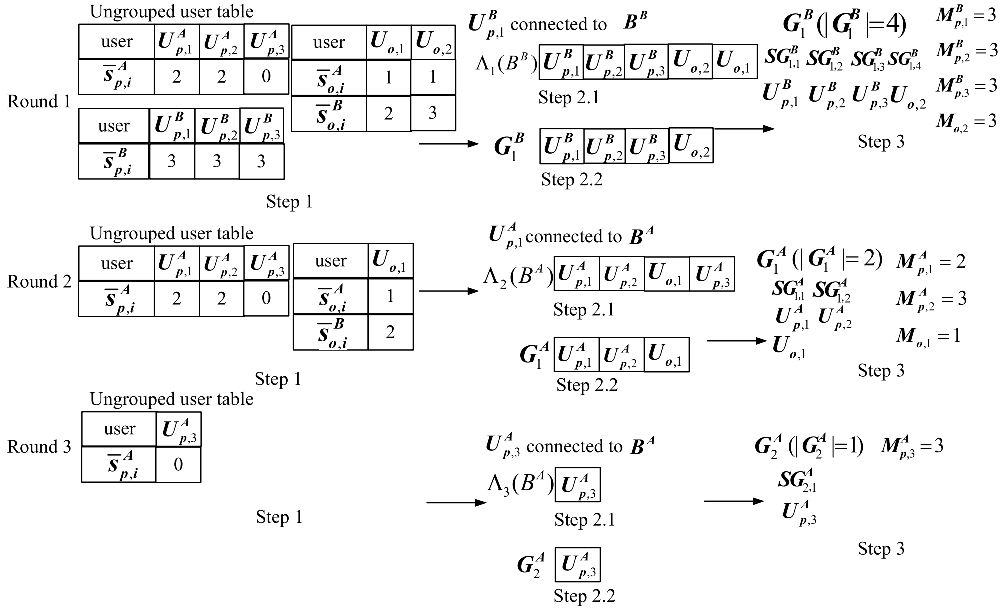

FIGURE 7. Example of joint optimization of transmitter connection and user grouping.

connected transmitter for the group G_g^T in this round. When a private-user has the same maximum SNR reduced factor as an overlapped-user, the private-user and its connected transmitter are selected with the higher priority, because overlapped-users have more transmitters which to connect. When different users have the same maximum SNR reduced factor, we randomly choose one of these users and its connected transmitter. After the first user in G_g^T and its connected transmitter B^T are selected, the users who can connect to B^T within the ungrouped user table can be presented a set $\Lambda_g(B^T)$ (including B^T's private-users and all overlapped-users). The users in $\Lambda_g(B^T)$ are further ranked based on their maximum SNR reduced factors with respect to B^T. For example in the first round in Fig. 7, $U_{p,i}^B$, $i = 1, 2, 3$, and $U_{o,2}$ for B^B have the same maximum SNR reduced factor, so we select $U_{p,1}^B$ as the first user in G_1^B and its connected transmitter is B^B. Then, B^B's private-users $U_{p,1}^B$, $U_{p,2}^B$ and $U_{p,3}^B$ along with all the overlapped-users in the ungrouped user table, form the set $\Lambda_1(B^B)$.

Step 2.2 (Allocate Users in $\Lambda_g(B^T)$ to Group G_g^T): We select the user U_i^T with the maximum $\bar{s}_i^T$ in $\Lambda_g(B^T)$ and check whether it can be added to G_g^T based on Proposition 1. If adding U_i to G_g^T will not reduce the number of subgroups in G_g^T (based on (31)) and if it is also ensure that U_i can be allocated at least one antenna of the transmitter (based on (32)), U_i is added to G_g^T. Otherwise, U_i is not included in G_g^T and is also removed from $\Lambda_g(B^T)$. The above two restrictions ensure that G_g^T can accommodate U_i, and that U_i can improve the overall DoF of G_g based on (28). *Step 2.2* is repeated until $\Lambda_g(B^T)$ becomes empty. For example, in the first round in Fig. 7, $U_{p,2}^B$, $U_{p,3}^B$ and $U_{o,2}$ are added to G_1^B because they can increase G_1^B's number of subgroups ($|G_1^B|$ is increased to 4 after U_{o2} is added to G_1^B) and also satisfy (32). After that, $U_{o,1}$ cannot join this group because its maximum SNR reduced factor connecting to B^B is $\bar{s}_{o3}^B = 2$. If $U_{o,1}$ joints G_1^B, based on (30), the number of subgroups in G_1^B will be $\bar{s}_{o3}^B + 1 = 3$, which is smaller than the number of subgroups when $U_{o,1}$ is not added to G_1^B.

3) STEP 3 (SUBGROUP ALLOCATION WITHIN GROUP)

The users in group G_g^T are further divided into $|G_g^T|$ subgroups, and $|G_g^T|$ can be calculated based on (29). Additionally, based on Theorem 1, how to allocate the user into subgroups does not affect the overall DoF, and the users can be equally allocated to different subgroups. The transmission scheme and receiving scheme in each group follow Fig. 4 in Section III. For example, in the second round, three users ($U_{p,1}^A$, $U_{p,2}^A$ and $U_{o,1}$) form G_1^A with $|G_1^A| = 2$ subgroups. The first two users in $G_{1,1}^A$ ($U_{p,1}^A$ and $U_{p,2}^A$) are allocated into the first and second subgroups. Since there are only two subgroups in G_1^A, the next user in G_1^A ($U_{o,1}$) is allocated into the first subgroup, i.e., $U_{p,1}^A$ and $U_{o,1}$ are in the same subgroup. Since the number of antennas belonging to the transmitter($M = 3$) cannot be evenly divided by 2, we allocate 2 antennas to $U_{p,1}^A$ and 1 antenna to $U_{o,1}$. Because $U_{p,2}^A$ independently forms the second subgroup, it occupies 3 antennas.

The above steps are repeated until the algorithm converges, which occurs when each user has been allocated into a group. This is because one ungrouped user is selected in Step 2.1 to form a group, and several ungrouped users are further added to this group in Step 2.2. Therefore, at least one ungrouped user can be allocated into a group in each round, and the algorithm converges with at most K rounds (K is the number

Algorithm 1 The Joint Optimization of Transmitter Connection and User Grouping Algorithm

Input:
  Ungrouped user table $\mathbf{U}$; the group index $g = 1$;
Output:
  The user grouping scheme;

```
while U is not empty do
    Select the first user in U and its corresponding transmitter B^T
    Form the users in U who can connect to B^T into Λ_g(B^T)
    while Λ_g(B^T) is not empty do
        if Adding the first user in Λ_g(B^T) (U_i^T) to G_g satisfies Proposition 1 and |G_g| is not reduced based on (29) then
            U_i^T is added to G_g and is removed from Λ_g(B^T)
        else
            U_i^T is removed from Λ_g(B^T)
        end if
    end while
    Determine |G_g| based on (29)
    Equally allocate the users in G_g into |G_g| subgroups
    Design the transmission scheme and receiving scheme of G_g based on Section III.B
    Update U and g = g + 1
end while
End algorithm.
```

of users). Moreover, such an algorithm is centrally performed at the transmitter and broadcasted at the beginning of a frame. Therefore, in practice, all users can follow the grouping result (including the corresponding transmission scheme and receiving scheme), decoding their individual desired EDSs.

The specific SNR BIA in two-cell network algorithm is as shown in AL. 1.

C. THE ACHIEVABLE SUM RATE ANALYSIS

In this subsection, we analyze the achievable sum rate of SNR BIA, which is given by the following theorem.

Theorem 2: In a two-cell network, if the two transmitters work in different channels, the achievable sum rate in SNR BIA by following zero-forcing interference at each user is

$$\begin{aligned} R_{\text{SNR BIA}} = & \frac{1}{2}\sum_{T=A,B}\sum_{U_i^T\in B^T} \\ & \times \frac{(M-1)^{|G_g^T|-1}}{\sum_{g=1}^{|G^T|}[(M-1)^{|G_g^T|}+|G_g^T|(M-1)^{|G_g^T|-1}]} \\ & \times \frac{M_i}{M}\mathbb{E}[\log\det(\mathbf{I}_M + P_e\mathbf{H}_i^T{\mathbf{H}_i^T}^{\dagger}\mathbf{R}_{\tilde{\mathbf{z}}_i^T}{}^{-1})], \end{aligned} \tag{36}$$

where $\mathbf{I}_M$ is the $M \times M$ identity matrix, $\mathbf{H}_i^T = [\mathbf{h}_i^T(1), \ldots, \mathbf{h}_i^T(M)]^{\dagger}$, P_e is the transmission power of each EDS, and

$$\mathbf{R}_{\tilde{\mathbf{z}}_i^T} = \begin{bmatrix} |G_g^T|\mathbf{I}_{M-1} & 0 \\ 0 & 1 \end{bmatrix}, \quad \forall U_i^T \in G_g^T. \tag{37}$$

Proof: Based on the transmission scheme in the user grouping framework, a specific user $U_i^T \in SG_{g,s}^T$ receives the subgroup's desired EDSs $\mathbf{X}_{g,s}^T$ together with $|G_g^T| - 1$ subgroup interference $M - 1$ times, in the overlapped part. Then, this user and independently receives $\mathbf{X}_{g,s}^T$ a single time in the independent part. In the overlapped part, $|G_g^T| - 1$ subtractions are required in the received equations and the noise power is increased $|G_g^T| - 1$ fold in each received equation. In the independent part, no subtraction is required and the noise power remains unchanged. Let $\tilde{\mathbf{z}}_i^T$ denote the noise of $U_i^T \in G_g^T$ after the interference elimination and $\tilde{\mathbf{z}}_i^T \sim \mathcal{CN}(0, \mathbf{R}_{\tilde{\mathbf{z}}_i^T})$ [19]. We have

$$\mathbf{R}_{\tilde{\mathbf{z}}_i^T} = \begin{bmatrix} |G_g^T|\mathbf{I}_{M-1} & 0 \\ 0 & 1 \end{bmatrix}. \tag{38}$$

U_i^T's achievable rate in one set of $\mathbf{X}_{g,s}^T$ with zero forcing can be written as

$$R_{i,EDS}^T = \frac{M_i^T}{M}\mathbb{E}[\log\det(\mathbf{I}_M + P_e\mathbf{H}_i^T{\mathbf{H}_i^T}^{\dagger}\mathbf{R}_{\tilde{\mathbf{z}}_i^T}{}^{-1})], \tag{39}$$

where $\frac{M_i^T}{M}$ indicates that M_i^T EDSs are intended for U_i^T in one set of $\mathbf{X}_{g,s}^T$. In addition, based on (19) and (26), $ES_{g,s}^T$ sets of EDSs intended for $U_i^T \in SG_{g,s}^T$ are transmitted within $\sum_{g=1}^{|G^T|} l_g^T$ slots. The achievable sum rate of all users in the two-cell network is

$$\begin{aligned} R_{\text{SNR BIA}} &= \frac{1}{2}\sum_{T=A,B}\sum_{U_i^T\in SG_{g,s}^T}\frac{ES_{g,s}^T}{\sum_g l_g^T}R_{i,EDS}^T \\ &= \frac{1}{2}\sum_{T=A,B}\sum_{U_i^T\in SG_{g,s}^T} \\ &\quad \times \frac{(M-1)^{|G_g^T|-1}}{\sum_{g=1}^{|G^T|}[(M-1)^{|G_g^T|}+|G_g^T|(M-1)^{|G_g^T|-1}]} \\ &\quad \times \frac{M_i^T}{M}\mathbb{E}[\log\det(\mathbf{I}_M + P_e\mathbf{H}_i^T{\mathbf{H}_i^T}^{\dagger}\mathbf{R}_{\tilde{\mathbf{z}}_i^T}{}^{-1})], \end{aligned} \tag{40}$$

where $\frac{1}{2}$ means that the two cells work at two different frequencies.

Remark: From the above analysis, the achievable sum rate improvement lies in two aspects. First, based on the SNR BIA framework, each user's SNR reduced factor is decreased, leading to the increased transmission rate on each EDS especially for the users with lower rSNRs. Besides, the transmitter connection and user grouping scheme are joint optimized. That is, through selecting the transmitters for overlapped-users, these users can have superior rSNRs. They can be further allocated into groups with the other private-users for the improved overall eDoF.

V. PERFORMANCE EVALUATIONS

We compare the multi-cell SNR BIA (denoted SNR BIA) with the other typical BIA mechanisms including standard BIA (sBIA) [6], data shared BIA (dBIA) [16], and extended BIA (eBIA) [17] in a two-cell network. Because these BIAs are not designed for a multi-cell network with different frequencies, they are modified to adapt to our scenario for performance comparisons. Specifically, we assume that all overlapped-users are equally divided into two cells in sBIA for load balance. In eBIA and dBIA, two transmitters need to work cooperatively (two transmitters work as a unit in eBIA and encode EDSs together in dBIA) for transmitting EDSs to all users in one frequency. Therefore, they can achieve twice the DoFs in our scenario, compared with the scenario in which they work in one frequency.[7]

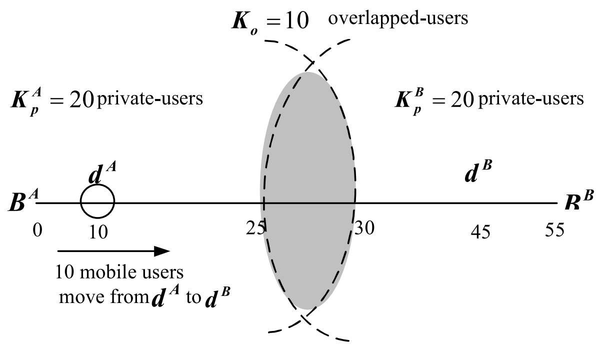

FIGURE 8. Two-cell network evaluation scenario.

The simulation scenario is deployed as shown in Fig. 8, where the transmitters B^A and B^B each have three antennas ($M = 3$). The coverage of each cell is assumed to be a circle with a radius of 30 meters, and the distance between B^A and B^B is 55 meters [17], forming the overlapped area shown in Fig. 8. Each transmitter connects 20 private-users ($K_p^A = K_p^B = 20$) who are randomly distributed in the non-overlapping area, and 10 overlapped-users are randomly distributed within the overlapped area. The transmission power for one transmitted EDS is assumed to be $P_e = -15$ dBm, and the noise power at each transmitter is set to be -104 dBm [20]. The channel between one transmitter and one user is modeled as follows. The path loss effect follows the model $PL(d_i^T) = 15.3 + 37.6 \log d_i^T$, where d_i^T is the distance between U_i and B^T. The small scale fading effect follows the Rayleigh distribution with $\mathcal{CN}(0, 1)$ [17]. The SNR threshold SNR_{th} is selected to be 15 dB, which can be used as a coarse-grained measurement of the channel quality [21]. 1000 experimental runs are performed for each simulation scenario.

Fig. 9 shows the CDFs of the eDoF and the achievable sum rate. It can be observed that the 80th percentile of SNR BIA's eDoF (achievable sum rate) distribution is

[7] We do not consider the additionally cooperative cost when eBIA (dBIA) is modified adapting to our scenario. In theory, eBIA (dBIA) can achieve twice DoFs when its bandwidth is doubled.

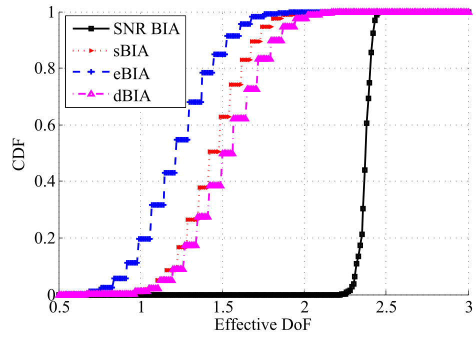

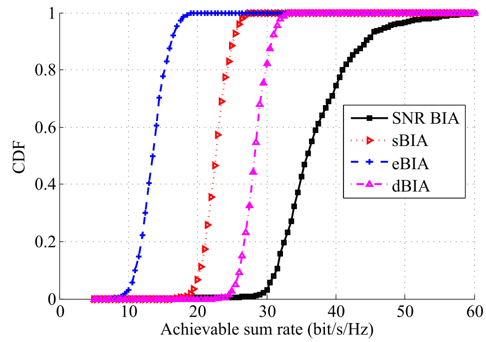

FIGURE 9. CDF of Performances. (a) Effective DoF. (b) Achievable sum rate.

approximately 2.43 (40.5 bit/s/Hz), which is 1.38 times (1.36 times), 1.47 times (1.66 times), and 2.7 times (2.68 times) those of dBIA, sBIA, and eBIA, respectively. This performance improvement is achieved by SNR BIA considering the rSNRs of the users and transmitter connections together. First, the user grouping scheme can reduce users' SNR reduced factors to improve their eDoF and the achievable sum rate in each EDS. Moreover, the joint optimization of the user grouping scheme and the transmitter connection can aggregate the users with similar rSNRs into a group, so that the number of subgroups can be as large as possible. However, the other BIA mechanisms do not limit the rSNR deterioration. The reduced fSNRs result in reduced eDoFs and severely reduce the achievable sum rates although they can achieve high DoFs. Additionally, they do not consider the transmitter connection problem in the multi-cell scenario, and inappropriate transmitter connections can negatively influence their eDoFs and achievable sum rates.

We consider the impact of SNR_{th} on performances within the range [10 dB, 20 dB] in Fig. 10. Generally, fSNR below 10 dB cannot support the available EDS decoding. The channel with the fSNR above 20 dB can be regarded as the high-SNR channel [21]. As SNR_{th} increases, the eDoFs of sBIA, eBIA and dBIA decrease sharply, as shown in Fig. 10(a), but SNR BIA's eDoF decreases in a more subtle way. This is because the higher SNR_{th} means that higher fSNR is required for contributing one eDoF and each group can

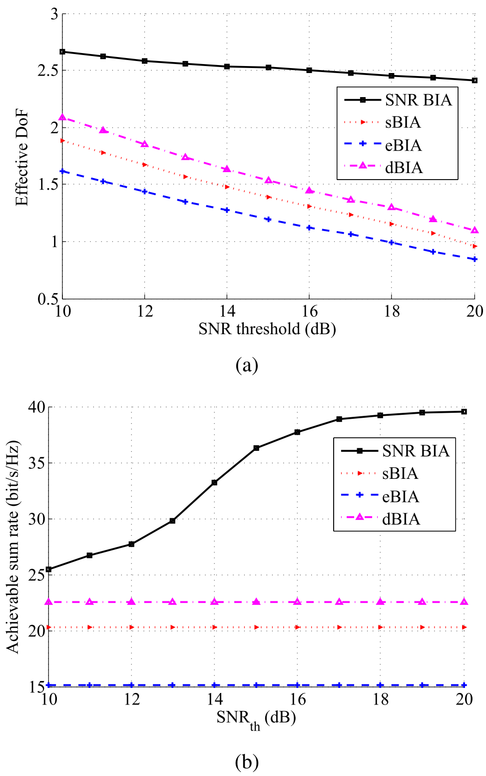

FIGURE 10. **The impact of SNR threshold on the performances. (a) The impact of SNR threshold on effective DoF. (b) The impact of SNR threshold on achievable sum rate.**

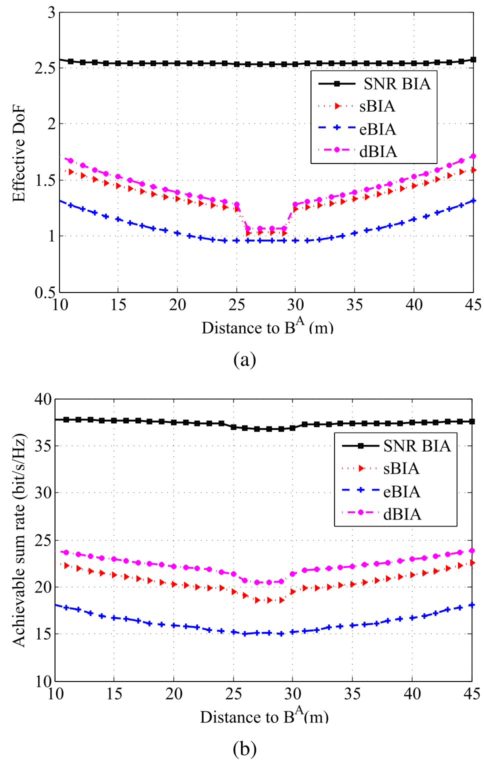

FIGURE 11. **Impact of mobility on performances. (a) Effective DoF. (b) Achievable sum rate.**

include fewer users to ensure that their SNR reduced factors remain above SNR_{th}. SNR BIA can adjust the transmitter connection and the user grouping scheme for optimizing eDoF with the SNR_{th} constraints. The users with higher rSNRs can form one group with more users contributing more to the eDoF performance, while the users with smaller rSNRs can form another group with fewer users, ensuring that their transmitted EDSs all contribute to the eDoF performance. That is, SNR BIA can adapt to the change in SNR_{th} and optimize the overall eDoF as much as possible. However, the SNR reduced factor is not considered in the other BIA mechanisms. When SNR_{th} increases, fewer users' fSNRs are above SNR_{th}, and the eDoFs of these BIA mechanisms decrease rapidly.

Correspondingly, the achievable sum rate in SNR BIA first increases and then tends to be flat as shown in Fig. 10(b). This is because the SNR_{th} increase corresponds to the fSNR increase, leading to the increased achievable rate in each EDS. Although the increased SNR_{th} will also result in reduced eDoF, the positive impact of the increased fSNR is more dominant. Therefore, the achievable sum rate increases as SNR_{th} increases. After SNR_{th} further increases above 17 dB, the decrease in the number of EDSs offsets the increase of the achievable rate in each EDS. Therefore, SNR BIA's overall achievable sum rate tends to be flat. However, the other BIA mechanisms do not adapt to SNR_{th}, so their achievable sum rates remain at the low level.

We further consider the adaptability mobility of different BIA mechanisms. In the above simulation scenario, we added 10 extra users moving from d^A (10 m away from B^A) to d^B (10 m away from B_B, 45 m from B_A) in a moving circle with a 3 m radius, as shown in Fig. 8. Fig. 11 shows the eDoFs and achievable sum rates when the users are in different locations. The x axis is the distance between the center of moving circle and B^A. As the distance between the users and B^A gradually increases, the users' space distribution and their rSNRs adapt to the change. It can be observed that SNR BIA has a higher and more stable eDoF (achievable sum rate) curve than the other BIA mechanisms. This is because, in the user grouping method, one subgroup can contain multiple users (at most M users). When the rSNRs of the mobile users (the distances between the mobile users and the transmitters change) decrease, SNR BIA can reduce the negative impact by adding the mobile users to the existing groups, instead of forming one new group. Moreover, the users' connections are also considered, to connect the mobile users to the transmitters which can have better performance. Therefore, the user grouping result for maximizing the overall eDoF changes as the users move. However, the other three mechanisms are static within each cell, even though both cells can be greatly affected by the users' distribution in space.

VI. CONCLUSION

Focusing on the noise accumulation phenomenon of BIA in multi-cell networks, this paper first presents a user grouping scheme for reducing noise accumulation in a single cell. That is, BIA is performed at the subgroup level so that the interference caused by all users in one subgroup is subtracted together, reducing their SNR reduced factors. We further analyze the impact of transmitter connections on the user grouping scheme, and propose a heuristic algorithm of the SNR BIA in the multi-cell network, which jointly optimizes transmitter connections and the user grouping scheme. Extensive simulations demonstrate that the effective DoF of SNR BIA is approximately 1.47 times, 2.7 times, and 1.38 times those of sBIA, eBIA, and dBIA, respectively, while the achievable sum rate of SNR BIA is approximately 1.66 times, 2.68 times, and 1.36 times those of sBIA, eBIA, and dBIA, respectively.

REFERENCES

[1] S. A. Jafar, *Interference Alignment: A New Look at Signal Dimensions in a Communication Network*. Breda, The Netherlands: Now Publishers Inc., 2011.

[2] V. R. Cadambe and S. A. Jafar, "Interference alignment and degrees of freedom of the K-user interference channel," *IEEE Trans. Inf. Theory*, vol. 54, no. 8, pp. 3425–3441, Aug. 2008.

[3] C. M. Yetis, T. Gou, S. A. Jafar, and A. H. Kayran, "On feasibility of interference alignment in MIMO interference networks," *IEEE Trans. Signal Process.*, vol. 58, no. 9, pp. 4771–4782, Sep. 2010.

[4] M. Razaviyayn, G. Lyubeznik, and Z.-Q. Luo, "On the degrees of freedom achievable through interference alignment in a MIMO interference channel," *IEEE Trans. Signal Process.*, vol. 60, no. 2, pp. 812–821, Feb. 2012.

[5] S. A. Jafar, "Exploiting channel correlations—Simple interference alignment schemes with no CSIT," in *Proc. IEEE Conf. Global Telecom. (GLOBECOM)*, Miami, FL, USA, Dec. 2010, pp. 1–5.

[6] T. Gou, C. Wang, and S. Jafar, "Aiming perfectly in the dark-blind interference alignment through staggered antenna switching," *IEEE Trans. Signal Process.*, vol. 59, no. 6, pp. 2734–2744, Jun. 2011.

[7] S. A. Jafar, "Blind interference alignment," *IEEE J. Sel. Topics Signal Process.*, vol. 6, no. 3, pp. 216–227, Jun. 2012.

[8] S. H. Chae and S.-Y. Chung, "Blind interference alignment for a class of K-user line-of-sight interference channels," *IEEE Trans. Commun.*, vol. 60, no. 5, pp. 1177–1181, May 2012.

[9] Y. Lu and W. Zhang, "Blind interference alignment in the K-user MISO interference channel," in *Proc. IEEE Conf. Global Telecom. (GLOBECOM),* Atlanta, GA, USA, Dec. 2013, pp. 3464–3469.

[10] C. Wang, H. C. Papadopoulos, S. A. Ramprashad, and G. Caire, "Improved blind interference alignment in a cellular environment using power allocation and cell-based clusters," in *Proc. Int. Conf. Commun. (ICC)*, Kyoto, Japan, Jun. 2011, pp. 1–6.

[11] Q. Yang, T. Jiang, and Z. Zhou, "SNR aware heterogeneous blind interference alignment in MISO broadcast channel," in *Proc. IEEE Wireless Commun. Netw. Conf. (WCNC)*, Doha, Qatar, Apr. 2016, pp. 1–6.

[12] Y. Lu, W. Zhang, and K. B. Letaief, "Blind interference alignment with diversity in K-user interference channels," *IEEE Trans. Commun.*, vol. 62, no. 8, pp. 2850–2859, Aug. 2014.

[13] H. Yang, W. Shin, and J. Lee, "Grouping based blind interference alignment for K-user MISO interference channels," in *Proc. IEEE Int. Symp. Inf. Theory (ISIT)*, Hong Kong, Jun. 2015, pp. 2827–2831.

[14] H. Yang, W. Shin, and J. Lee, "Hierarchical blind interference alignment over interference networks with finite coherence time," *IEEE Trans. Signal Process.*, vol. 64, no. 5, pp. 1289–1304, Mar. 2015.

[15] S. Akoum, C. S. Chen, M. Debbah, and R. W. Heath, Jr., "Data sharing coordination and blind interference alignment for cellular networks," in *Proc. IEEE Conf. Global Telecom. (GLOBECOM)*, Anaheim, CA, USA, Dec. 2012, pp. 4273–4277.

[16] Y. Lu and W. Zhang, "Downlink blind interference alignment for cellular networks," in *Proc. IEEE Conf. Global Telecom. (GLOBECOM)*, Austin, TX, USA, Dec. 2014, pp. 3337–3342.

[17] F. C. Kavasoglu, Y. Huang, and B. D. Rao, "Semi-blind interference alignment techniques for small cell networks," *IEEE Trans. Signal Process.*, vol. 62, no. 23, pp. 6335–6348, Dec. 2014.

[18] M. Morales-Céspedes, J. Plata-Chaves, D. Toumpakaris, S. A. Jafar, and A. G. Armada, "Blind interference alignment for cellular networks," *IEEE Trans. Signal Process.*, vol. 63, no. 1, pp. 41–56, Jan. 2015.

[19] C. Wang, H. C. Papadopoulos, S. A. Ramprashad, and G. Caire, "Design and operation of blind interference alignment in cellular and cluster-based systems," in *Proc. IEEE Inf. Theory Appl. Workshop (ITA)*, La Jolla, CA, USA, Feb. 2011, pp. 1–10.

[20] J. Ahmed, A. Hussain, M. Y. Siyal, H. Manzoor, and A. Masood, "Parametric analysis of four wave mixing in DWDM systems," *Opt.-Int. J. Light Electron Opt.*, vol. 125, no. 7, pp. 1853–1859, Apr. 2014.

[21] J. Yeo, M. Youssef, and A. Agrawala, "A framework for wireless LAN monitoring and its applications," in *Proc. 3rd ACM Workshop Wireless Secur.*, 2004, pp. 70–79.

QING YANG (S'15) received the B.S. degree from the Beijing University of Posts and Telecommunications in 2010. She is currently pursuing the PhD degree with the Key Laboratory of Universal Wireless Communication, Ministry of Education, Beijing University of Posts and Telecommunications, Beijing, China. Her current research interest is in interference alignment and signal processing.

TING JIANG received the B.S., M.S., and Ph.D. degrees in communication and information system from Yanshan University, China, in 1982, 1988, and 2003, respectively. He is currently a Professor with the Beijing University of Posts and Telecommunications. His research interests include the wireless broadband interconnection, the information theory, the short distance wireless communication technological theory and application, and the wireless sensor network.

CHUNXIAO JIANG (S'09–M'13–SM'15) received the B.S. degree (Hons.) in information engineering from Beihang University, Beijing, in 2008 and the Ph.D. degree (Hons.) in electronic engineering from Tsinghua University, Beijing, in 2013. He is currently an Assistant Research Fellow with the Tsinghua Space Center, Tsinghua University. He has authored/co-authored over 100 technical papers in renowned international journals and conferences, including over 50 renowned IEEE journal papers. He has been actively involved in organizing and chairing sessions. His research interests include application of game theory, optimization, and statistical theories to communication, networking, signal processing, and resource allocation problems, in particular space information networks, heterogeneous networks, social networks, and big data privacy. He has served as a member of the Technical Program Committee and the Symposium/Workshop Chair for a number of international conferences. He is currently an Editor for the Wiley Wireless Communications and Mobile Computing, the Wiley Security and Communications Networks, and the *I*nternational Journal of Big Data Intelligence, and a Guest Editor for the *A*CM/Springer Mobile Networks and Applications Special Issue on Game Theory for 5G Wireless Networks. He was a recipient of the best paper award from the IEEE GLOBECOM in 2013, the Best Student Paper Award from the IEEE GlobalSIP in 2015, the Distinguished Dissertation Award from the Chinese Association for Artificial Intelligence in 2014, and the Tsinghua Outstanding Postdoc Fellow Award (only ten winners each year) in 2015.

ZHU HAN (S'01–M'04–SM'09–F'14) received the B.S. degree in electronic engineering from Tsinghua University in 1997, and the M.S. and Ph.D. degrees in electrical and computer engineering from the University of Maryland, College Park, in 1999 and 2003, respectively. From 2000 to 2002, he was a Research and Development Engineer with JDSU, Germantown, Maryland. From 2003 to 2006, he was a Research Associate with the University of Maryland. From 2006 to 2008, he was an Assistant Professor with Boise State University, Idaho. He is currently a Professor with the Electrical and Computer Engineering Department and the Computer Science Department, University of Houston, Texas. His research interests include wireless resource allocation and management, wireless communications and networking, game theory, big data analysis, security, and smart grid. He received an NSF Career Award in 2010, the Fred W. Ellersick Prize of the IEEE Communication Society in 2011, the EURASIP Best Paper Award for the Journal on Advances in Signal Processing in 2015, the IEEE Leonard G. Abraham Prize in the field of Communications Systems (best paper award in the IEEE JSAC) in 2016, and several best paper awards in the IEEE conferences. He is currently an IEEE Communications Society Distinguished Lecturer.

ZHENG ZHOU (M'05) received the bachelor's degree in electrical engineering from the Harbin Institute of Military Engineering, Harbin, China, in 1967, and the master's and Ph.D. degrees in electrical engineering from the Beijing University of Posts and Telecommunications (BUPT), Beijing, China, in 1982 and 1988, respectively. He was a Visiting Research Fellow with the Information Engineering Department, Chinese University of Hong Kong, Hong Kong, from 1993 to 1995. He was also the Vice-Dean with the School of Telecommunication Engineering, BUPT, from 1998 to 2003, and was the invited overseas Researcher with the Japan Kyocera DDI Future Communication Research Institute (supported by the Japan Key Technology Center) in 2000. He is currently a Professor with the Beijing University of Posts and Telecommunications, Beijing, China. He was a member of the Technical Subcommittee on Cognitive Networks, the IEEE Communications Society, the International Steering Committee Member of the IEEE International Symposium on Communications and Information Technologies (ISCIT) from 2003 to 2010, and the TPC Co-Chair of the IEEE ISCIT 2005. He was also the General Vice Chair of the IEEE ChinaCom 2006 (the first international conference on communications and networking in China), and the Steering Committee Member of the IEEE ChinaCom 2007. He is a Voting Member and Contributor of the IEEE 802.15 Task Group (TG3a and TG4a), a Senior Member of the China Institution of Communications (CIC), the Radio Application and Management Technical Committee Member of CIC, a Senior Member of the China Computer Federation (CCF), a Sensor Network Technical Committee Member of CCF, an H-Subcommittee Member of the China Radio Interference Standard Technology Committee, the General Secretary of the China UWB Forum, and the General Secretary of the China Bluetooth Forum.